

Hydrothermal alteration and magnetic properties of rocks in the Carolina de Michilla stratabound copper district, northern Chile

Brian Townley · Pierrick Roperch · Verónica Oliveros ·
Andres Tassara · César Arriagada

Received: 12 February 2006 / Accepted: 14 March 2007 / Published online: 8 May 2007
© Springer-Verlag 2007

Abstract In the Carolina de Michilla district, northern Chile, stratabound copper mineralization is hosted by Jurassic volcanic rocks along the trace of the Atacama fault system. In this study, we present the overall effects of hydrothermal alteration on the magnetic properties of rocks in this district. Two types of metasomatic alteration associations occur, one of regional extent and the other of local hydrothermal alteration associated with copper mineralization (e.g., Lince–Estefanía–Susana). Regional alteration is interpreted as a low-grade “propylitic association” characterized by an epidote–chlorite–smectite–titanite–albite–quartz–calcite association. The local hydrothermal alteration is characterized broadly by a quartz–albite–epidote–chlorite–calcite mineral assemblage. The most pervasive alteration mineral is albite, followed by epidote and, locally, actinolite. These minerals contrast sharply against host rock minerals such as chlorite, calcite, zeolite, prehnite, and pumpellyite, but alteration is constrained to mineralized bodies as narrow and low contrast alteration halos that go outwards from actinolite–albite to epidote–albite, to epidote–chlorite, and finally to chlorite. Hydrothermal alteration minerals, compared to regional alteration minerals, show iron-rich epidotes, a lower chlorite content of the chlorite–smectite series, and a nearly total albite replacement of plagioclase in the mineralized zones. Opaque minerals associated with

regional alteration are magnetite and maghemite, and those associated to hydrothermal alteration are magnetite, hematite, and copper sulphides. We present paleomagnetic results from nine sites in the Michilla district and from drill cores from two mines. Local effects of hydrothermal alteration on the original magnetic mineralogy indicate similar characteristics and mineralogy, except for an increase of hematite that is spatially associated with the Cu–sulphide breccias with low magnetic susceptibilities. Results indicate that it is impossible to magnetically differentiate mineralized bodies from unmineralized lavas, except for pyrite-rich hydrothermal breccias. In conclusion, for stratabound copper deposits of the Michilla type, the overall effect of hydrothermal alteration on the paleomagnetic properties of rocks is of low contrast, not clearly discernable even at a small scale. From an exploration point of view, magnetic exploration surveys should not discern mineralized bodies of Cu–sulphide breccias except in detailed ground surveys due to the small size of contrasting bodies. Unoriented drill cores with primary ore mineralization record a characteristic remanent magnetization of reverse polarity. Taking into account the azimuth and dip of the drill cores, we were able to compare the magnetization of the mineralized bodies with the characteristic directions from sites drilled in situ from Late Jurassic–Early Cretaceous intrusives mostly. The characteristic direction recorded by the Pluton Viera is similar to the magnetization of the ore bodies of the Estefanía mine. If copper mineralization mostly postdates the tilt of the volcanic flows, the low paleomagnetic inclinations suggest an age for the mineralization near 145 Ma, the time of the lowest paleolatitude for the South American plate during the Mesozoic.

Editorial handling: B. Lehmann

B. Townley (✉) · V. Oliveros · A. Tassara · C. Arriagada
Departamento de Geología, Universidad de Chile,
P.O. Box 13518, Correo 21,
Santiago, Chile
e-mail: btownley@cec.uchile.cl

P. Roperch
IRD, UR154 LMTG and Géosciences Rennes,
Rennes, France

Keywords Hydrothermal alteration · Rock magnetic properties · Stratabound Cu mineralization · Chile

Introduction

Hydrothermal alteration and mineralization processes imply changes within the host-rock mineralogy, either by metasomatism of pre-existing minerals or by growth of neo-formed alteration minerals. The alteration or crystallization of “ferromagnetic” minerals suggests changes in the magnetic properties of such affected rocks, hence, a magnetic contrast between altered and unaltered rocks. In this paper, we present the results of a study of hydrothermal alteration and the related effects on magnetic properties in rocks of the Carolina de Michilla district, northern Chile (Fig. 1). In this district, Jurassic volcanic rocks are host to stratabound copper mineralization (e.g., Susana, Lince, Estefania) that is spatially associated with the trace of the Atacama fault system (Fig. 2).

Copper exploration along the “metallogenic belt of the Coastal Cordillera” (Boric et al. 1990) is active, and the potential for finding additional mineralization remains. Poor quality of outcrops and a high proportion of Cenozoic and recent gravel cover have justified the use of geophysical exploration techniques, including airborne and ground magnetic surveys among others. Magnetometry, despite being a potentially useful exploration tool, can benefit greatly from a better understanding of the magnetic properties of the rocks and the contrast of these properties between altered and unaltered rocks. Data interpretation and modeling of magnetometric surveys do not usually take into account the specific magnetic properties of rocks such as the natural remanent magnetization (NRM) and magnetic susceptibility (k), fundamental parameters for the interpretation of magnetic anomalies. Interpretations that do not consider these parameters, or at least a realistic approximation, have a higher degree of uncertainty as noted by Roperch and Chauvin (1997).

Geological and metallogenic background

Stratabound copper deposits along the northern Coastal Cordillera of Chile are mainly hosted within Jurassic volcanic rocks of the La Negra Formation, as formally defined by García (1967). Multiple regional geologic studies have focused on these rocks, and the reader is referred to publications such as those presented by Naranjo and Puig (1984), Rogers (1985), Muñoz et al. (1988), Buchelt and Tellez (1988), Boric et al. (1990), and Marinovic et al. (1995). A brief summary is presented in this paper.

The volcanic sequence of the La Negra Formation crops out along the Coastal Cordillera between the cities of Arica and Taltal (10–26°S), with an estimated thickness of 3,500 to 7,000 m and a general homoclinal N–S strike and a dip

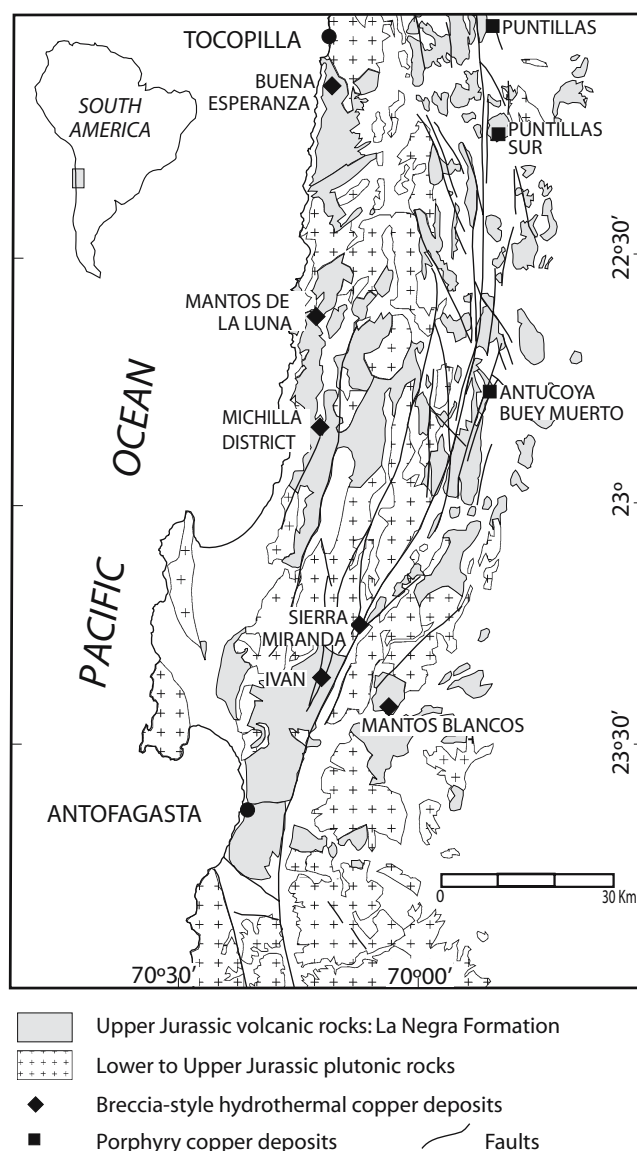
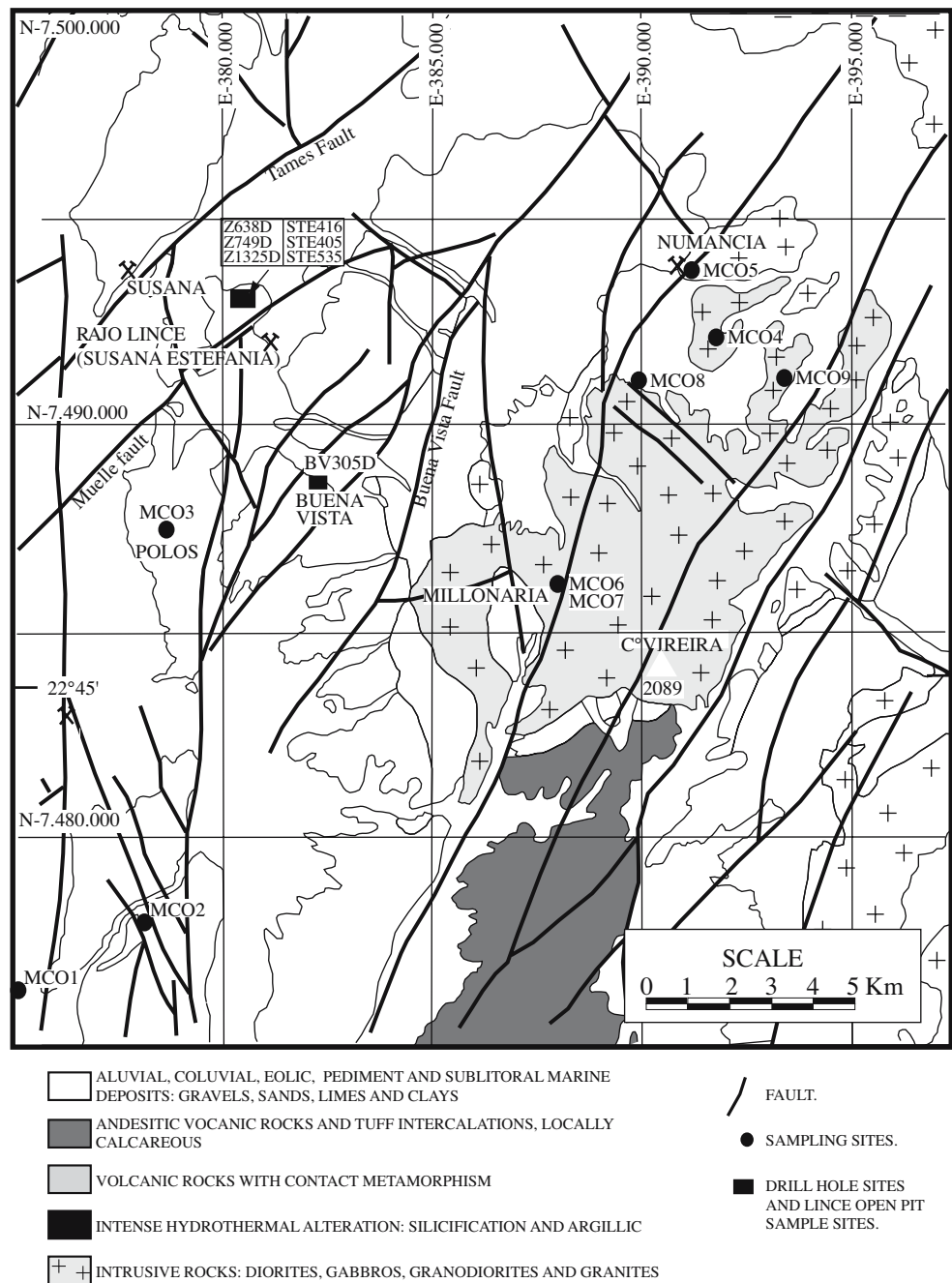


Fig. 1 Location of the Carolina de Michilla district and simplified regional geologic map of the Coastal Cordillera. Modified after Makshev and Zentilli (2002)

of 25–35°E, excluding important local variations. Figure 1 shows the distribution of these rocks together with other geologic units present between 22 and 24°S. Rocks of this formation consist mainly of basalt, andesitic–basalt, and andesite lava flows interstratified with less prominent volcanogenic clastic sedimentary and minor sandstone, shale, and limestone (some fossiliferous) sequences. Numerous dikes, sills, and small stocks locally intrude these volcanic rocks.

The base of the La Negra Formation concordantly overlies and, in part, laterally interdigitizes with Hettangian–Sinemurian marine sedimentary units such as the Pan de Azúcar (Naranjo and Puig 1984; Marinovic et al. 1995) and Cerro de Cuevitas (Muñoz et al. 1988) formations. The

Fig. 2 Sampling sites within the Carolina de Michilla district and simplified geology. Modified from Oliveros (2002)



La Negra Formation is thought to be discordantly overlain by the Tithonian–Neocomian Caleta Coloso Formation (Muñoz et al. 1988). Stratigraphic relationships indicate that the La Negra volcanics were deposited throughout most of the Jurassic, consistent with the radiometric ages for the lavas (Rb/Sr isochron of 186 ± 14 Ma, Rogers 1985; K/Ar of 160 ± 4 Ma, Marinovic et al. 1995; and $^{40}\text{Ar}/^{39}\text{Ar}$ 159.9 ± 1.1 Ma, Oliveros 2005) of subvolcanic intrusives (K/Ar of 165 and 133 Ma, Boric et al. 1990, and $^{40}\text{Ar}/^{39}\text{Ar}$ 159.6 ± 1.1 , 145 ± 3 and 137 ± 1 Ma, Oliveros 2005) and of gabbros, diorites, and granodiorites that are most probably cogenetic with the volcanic rocks. The distributions of both

the volcanic and intrusive rocks are spatially related to the geometry of the Atacama fault system (Fig. 1).

A distinctive characteristic of these volcanic rocks is a “low-grade regional metamorphism” that affects most of the sequence (Aguirre et al. 1999). This event has also been interpreted as a regional hydrothermal alteration associated with widespread volcanism and plutonism (Losert 1973). The regional metamorphism has a characteristic mineralogy composed of epidote, chlorite, calcite, chalcedony, albite, zeolites, prehnite, and pumpellyite, and it is mainly observed in high permeability rocks such as amigdaloidal and brecciated lavas. Based on apatite fission track and

$^{40}\text{Ar}/^{39}\text{Ar}$ thermochronology, Makshev (2000) concluded that rocks from this plutonic–volcanic arc were never deeply buried and have not been significantly uplifted or eroded since the Early Cretaceous, precluding to a great extent the possibility of a regional “low-grade metamorphism.”

Metallogenic overviews for the volcanic rocks of the La Negra Formation are given in detail by Boric et al. (1990), Espinoza et al. (1996), Vivallo and Henríquez (1998), and Makshev and Zentilli (2002). Within this metallogenic belt, the most outstanding deposit is Mantos Blancos, followed by smaller deposits such as Buena Esperanza, Mantos de La Luna (Fig. 1), and those within the Carolina de Michilla district (Fig. 2). These stratabound copper deposits consist, in general, of numerous ore bodies of various shapes such as mantoes, breccia pipes, and irregular bodies that are spatially associated with subvolcanic, mostly unmineralized, mafic intrusives. Mineralization consists mainly of atacamite and chrysocolla in the supergene oxidized upper portion of these deposits, and sulphides (chalcocite, bornite, covellite, and chalcopyrite, in some cases associated with hematite) in deeper primary ore as primary and secondary fracture fillings with lesser dissemination in breccias.

Despite controversy regarding the genetic interpretation of the mineralization in the stratabound copper deposits, the most widely accepted hypothesis supports an epigenetic origin related to the intrusion of dioritic stocks and dikes in the volcanic rocks (cf. Makshev 2000; Espinoza et al. 1996; Soto and Dreyer 1985; Sato 1984; Palacios and Definis 1981). Vivallo and Henríquez (1998) suggest that these stratabound deposits are linked to the genesis of the Cu–Fe veins that are widespread in this coastal metallogenic belt and that both types of deposits represent different levels within a magmatically associated hydrothermal system.

Geology of the Carolina de Michilla district

Rocks present within the Carolina de Michilla district consist of andesitic and andesitic–basalt lava flows, breccias and minor tuffs of the Jurassic La Negra Formation (Fig. 2). Upper portions of the lava flows are characteristically porous and brecciated in parts, whereas middle and lower portions are porphyritic to aphanitic in texture. On the western and eastern edges of the district, the volcanic rocks are intruded by the Coastal Batholith, comprised of gabbroic, monzonitic, and granodioritic plutons. Both volcanic and plutonic rocks are intruded by lesser subvolcanic porphyritic stocks, dikes, and sills of gabbroic to granodioritic composition. These subvolcanic bodies are often spatially associated with stratabound volcanic-hosted ore deposits (Soto and Dreyer 1985) and with vein-type ore mineralization hosted within the batholith (Venegas and Vergara 1985).

The most outstanding structural feature within the district is the Atacama fault zone, locally represented by the N–S Mititus and NE–SW Tames fault systems (Fig. 2). The spatial distribution and geometry of the intrusives and the locations of ore deposits coincide with these faults (Niemeyer et al. 1990; Venegas et al. 1991). The largest known ore bodies are located at and adjacent to major fault intersections.

Hydrothermal alteration and mineralization

Two types of metasomatic alteration associations occur within rocks of the Carolina de Michilla district, each associated with different alteration events. One is of distrital to regional extent that affects all rocks of the La Negra Formation, i.e., regional alteration. The second is localized and exclusively associated with copper mineralization, i.e., hydrothermal alteration.

The characterization of the hydrothermal alteration and mineralization presented in this study is based on the macroscopic description of sample sites (9), drill core log data (8 drill holes), and 67 and 420 paleomagnetic samples from sampling sites and drill hole cores, respectively (see Tables 1 and 2). From these samples, a total of 40 were selected for thin-section preparation and micropetrographic mineral characterization from which 15 were selected for mineral composition analysis using a JEOL 8900 superprobe at the University of New York, Binghamton. The microprobe operating conditions were, for the most part, 15 kV accelerating potential, 30 nA current, and a minimum spot size of <1 μm . The counting time for most elements was 30 s on peak and 10 s each on the upper and lower background positions. Na and K were counted for 10 s on peak and 5 s on background. The standards used include single-element oxides (Al, Si, Ti, and Fe). Amelia albite was used for Na. Orthoclase, MAD-10, was used for K. Diopside was used for Mg and Ca. Spessartine garnet was used for Mn. The mineral standards were all from C.M. Taylor. The standards were tested against various secondary standards from the Smithsonian Institution, as well as against internal standards. The total error based on the representative analyses of the samples was below 10% for most elements.

In addition, the description of hydrothermal alteration also incorporates detailed data from other studies, including micropetrographic and microprobe mineral composition analyses by Oliveros (2002).

Regional alteration

In general terms, the regional alteration is interpreted to be a low-grade propylitic association (Espinoza et al. 1996) or prehnite–pumpellyite facies metamorphism (Aguirre et al. 1999). This alteration type is characterized by an epidote–

Table 1 Sampling site data

Sample site	Number of samples	Rock type	Location	North UTM	East UTM	Elevation m.a.s.l.
MC01	8	Altered andesitic lavas, Cu oxide mineralization	Altar, San Porfirio Mine	7,476,003	373,759	1,216
MC02	7	Unaltered andesitic dike, 10 m	Between San Porfirio and Maria Luisa	7,478,619	378,412	1,005
MC03	7	Altered lavas and volcanic breccias Cu oxide mineralization	Polos Danae	7,487,720	378,770	941
MC04	6	Unaltered amphibole-pyroxene monzogranite, spheroidal weathering	Vireira Pluton	7,493,685	394,331	1,364
MC05	7	Andesitic lavas with variable degrees of contact metamorphism Cu oxide mineralization	Numancia Mine	7,493,930	389,920	1,469
MC06	9	Phaneritic to porphyritic granodiorite and diorite	Millonaria Mine	7,485,750	384,981	1,473
MC07	8	Amphibole and pyroxene monzo- and syeno-granites	Millonaria Mine	7,485,845	384,878	1,545
MC08	7	Fine grained tonalite and monzogranite	Vireira Pluton	7,491,462	391,521	1,383
MC09	8	Amphibole granite and monzogranite	Vireira Pluton	7,491,089	393,507	1,350

UTM Universal Transverse Mercator

chlorite–smectite–titanite–albite–quartz–calcite association that is common to all samples from the district. Epidote, in particular, is widespread within the volcanic rocks, and it is present in some cases as a pervasive replacement of lava beds, or most commonly as vug filling and disseminated clusters in the groundmass, or associated with hematite–limonite. Microprobe analysis of these alteration minerals indicates Fe-rich epidote and pistacite. Chlorite is also widespread within the volcanic rocks, mainly as vug fillings, as mafic mineral replacement, or as disseminated clusters in the groundmass, or in some rare cases as veinlets. The habit and color of the chlorites vary with location. The microprobe analyses indicate an Fe-rich composition (ripidolite, pycnochlorite, brunsvigite, and

lesser diabantite; Oliveros 2002). Albite is another common mineral in the regional alteration, mainly present as plagioclase selective replacement, be it either in phenocrysts or in microlites in the groundmass. In some cases, albite was also observed as vug fillings. The microprobe composition analysis shows Na-rich feldspars (5–10%) in exchange for low Ca (0.1–1%). The comparison of feldspar compositions between altered and unaltered rocks shows variations from $An_{2.3}-Ab_{97}-Or_{0.7}$ to $An_{55}-Ab_{43}Or_2$, respectively (Oliveros 2002), implying that regional alteration was driven in part by Na metasomatism. Iron oxides (mainly hematite), quartz, and chalcedony are widespread as vug fillings, veinlets in the groundmass, and phenocryst replacements. Opaque minerals such as magnetite and

Table 2 Exploration drill hole data

Drill hole	Number of samples	Rock type	Location	Length (m)	Az (degree)	Inclination (degree)
BV305D	182	Lavas and intrusives	Sector Buena Vista	250	155	–62
Z638D	78	Lavas, hydrothermal breccias and intrusives	Susana–Lince–Estefania	345	153	–55
Z749D	26	Mainly lavas	Susana–Lince–Estefania	191	172	0
Z1325D	38	Hydrothermal breccias and lavas	Susana–Lince–Estefania	80	336	–85
Z1324D	15	Lavas	Susana–Lince–Estefania	70	0	–90
STE416	32	Hydrothermal breccias and lavas	Susana–Lince–Estefania	55	0	90
STE405	31	Mainly intrusives	Susana–Lince–Estefania	80	77	0
STE535	18	Hydrothermal breccias and lavas	Susana–Lince–Estefania	25	352	0.5

maghemite occur as trace minerals, mainly within filled vug edges.

Hydrothermal alteration

Hydrothermal alteration related to copper mineralization shows a strong spatial relationship to lithology and permeability, both primary and secondary, that is reflected by weakly altered impervious porphyritic and aphanitic andesitic lavas interlayered with pervasively altered and mineralized porous amigdaloidal lavas and breccias (Fig. 3a and b). This lithologic permeability association of the mineralization is characteristic of stratabound copper deposits. A spatial relationship with structural permeability is also observed in terms of the location of the mineralization. In particular, it is associated with subvolcanic intrusives, stocks and dikes, which crosscut the deposits (Acevedo et al. 1997). Hydrothermal breccias also occur in which ore minerals form part of the breccia matrix (Fig. 3a). These breccias are genetically linked to the intrusion of subvolcanic bodies, and breccia fragments consist of host rock (lavas and volcanic breccia) and subvolcanic intrusives (Soto and Dreyer 1985; Palacios 1986; Wolf et al. 1990). All fragments have a common and characteristic “white alteration” that consists of pervasive albitization. Hydrothermal breccia bodies have a disseminated specular hematite halo that is up to 20 m in width. The mineralogical association observed in breccia matrix samples consists of albite, chlorite, titanite, sericite, epidote, and calcite, with minor apatite, actinolite, clay minerals, limonite, and gypsum. Alteration minerals observed in both hand samples and thin sections occur mainly as vug fillings, veinlets, primary mineral replacements, or volcanic breccia matrix replacement. In some cases, the latter is pervasive with total replacement of the matrix by quartz, albite, chlorite, titanite, and iron oxides. Figure 3 shows macroscopic, microscopic, and scanning electron microscopy (SEM) images of alteration aspects and minerals.

Hydrothermal alteration epidote has a composition that is Fe-rich, of the pistacite type, and has a pistacite content ($X_{\text{Fe}^{+3}}$) that is higher in these rocks than in the regional alteration epidote. Hydrothermal alteration phyllosilicates represent midmembers of the chlorite–smectite series, which in general, have lower chlorite compositions than those observed in the regional alteration and are mainly diabantite and pycnochlorite, hence, lower in SiO_2 and Fe content and richer in Mg content (Oliveros 2002). Hydrothermal alteration amphiboles include actinolite and magnesiohornblende, mainly as vug filling together with chlorite, quartz, albite, calcite, and hematite. Hydrothermal alteration albite observed in thin sections as a pervasive microlitic mineral in matrix and as a replacement of plagioclase is the most common and widespread alteration

mineral in these deposits. Metasomatism consists of plagioclase replacement (originally An_{40} and higher) by albite with a composition of up to $\text{An}_1\text{Ab}_{99}$. Minor sericitic alteration is common together with the albite. Magnetite and hematite are present as accessory alteration minerals, together with titanite and apatite. Both these minerals, in association with ore minerals, imply an oxidation trend from a magnetite–chalcopyrite–bornite buffer to a chalcocite–hematite buffer. Individual mineralized bodies have vertical zoning of the minerals from top to bottom, consisting of atacamite–chrysocolla–hematite (specular), chalcocite–covellite, chalcocite–bornite, and finally, chalcopyrite–bornite–pyrite.

Overall, the mineralogical differences in the alteration associations are not great between regional altered host rocks and hydrothermal altered ore rocks. Metasomatism in both cases is suggested to be Na–Fe-rich with oxidation trends. The magnetic minerals are magnetite that is present in both types of alteration, maghemite that is mostly the product of regional alteration and hematite that is mostly characteristic of hydrothermal alteration. The maghematization of magnetite that is observed in the ore rocks suggests that the regional alteration may postdate mineralization, as suggested by Wolf et al. (1990), based on crosscutting relationships of intrusives, alteration, and mineralization.

Paleomagnetic study

Paleomagnetic sampling

Figure 2 shows the locations of the nine sampling sites within the Carolina de Michilla district from which 67 paleomagnetic samples were taken (Tables 1 and 2). In addition, paleomagnetic minicore samples from eight exploration diamond drill holes of various lengths, orientations, and lithology (Fig. 4) were sampled for a total of 420 paleomagnetic samples. Seven exploration drill holes are within the Lince–Estefanía–Susana mine, and only one is from the Buena Vista sector (Tables 1 and 2, Fig. 2). Several paleomagnetic minicore samples were also drilled in situ within the Lince open pit. Tables 1 and 2 presents relevant data for each sampling site and exploration drill hole.

The core from drill holes BV305D and Z638D have a high-density systematic sampling (Fig. 4), while the core from the other drill holes were sampled selectively. The samples represent intrusive rocks (mainly dioritic), lava flows of different textures, and mineralized intercepts that are up to tens of meters long with hypogene (chalcocite) and mixed (atacamite–chrysocolla–chalcocite) ore mineralization in high primary permeability zones and high-grade hydrothermal breccias.

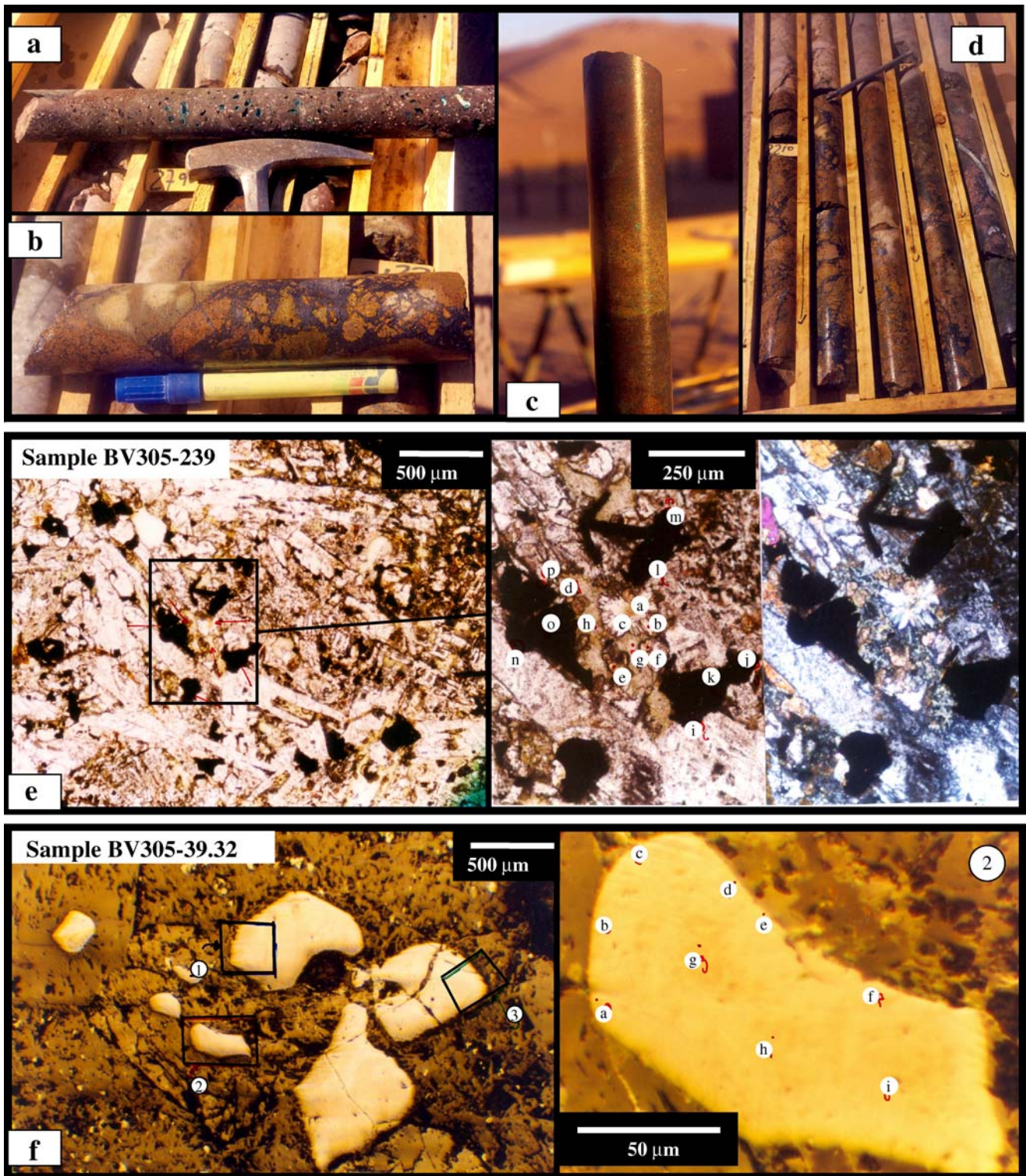


Fig. 3 a–d Drill core samples with copper mineralization infilling vesicles and as replacements within porous andesitic lavas (a and c), and chalcocite matrix mineralized hydrothermal breccias (b and d). e Microphotography of sample BV305.239, transmitted light. *Left* at 40× parallel nichols and *center right* at 100× parallel nichols, showing microprobe analytical points (a through p); *far right* at 100× crossed nichols. Hydrothermal alteration is represented by quartz, albite, smectite, and chlorite. Details of probe analysis are provided in g. f Microphotography of sample BV305.39.32, reflected light. *Left* at

40×, parallel nichols; *right* at 400× parallel nichols. Outlines 1, 2, and 3 indicate zones of probe analyses. *Right* represents zone 2, indicating probe analytical points (a through i). These opaque minerals represent magnetite cores surrounded by hematite (or maghemite) rims. Details of probe analysis are provided in g. g SEM image of samples BV305.239 (*left*) and BV305.39.32 (*right*). Analytical points are indicated as follows: BV305.239, a, d, and e quartz; b and c smectite; g albite; h chlorite; i–l, n–p magnetite–hematite (maghemite). BV305.39.32, a–f hematite or maghemite; g–h magnetite

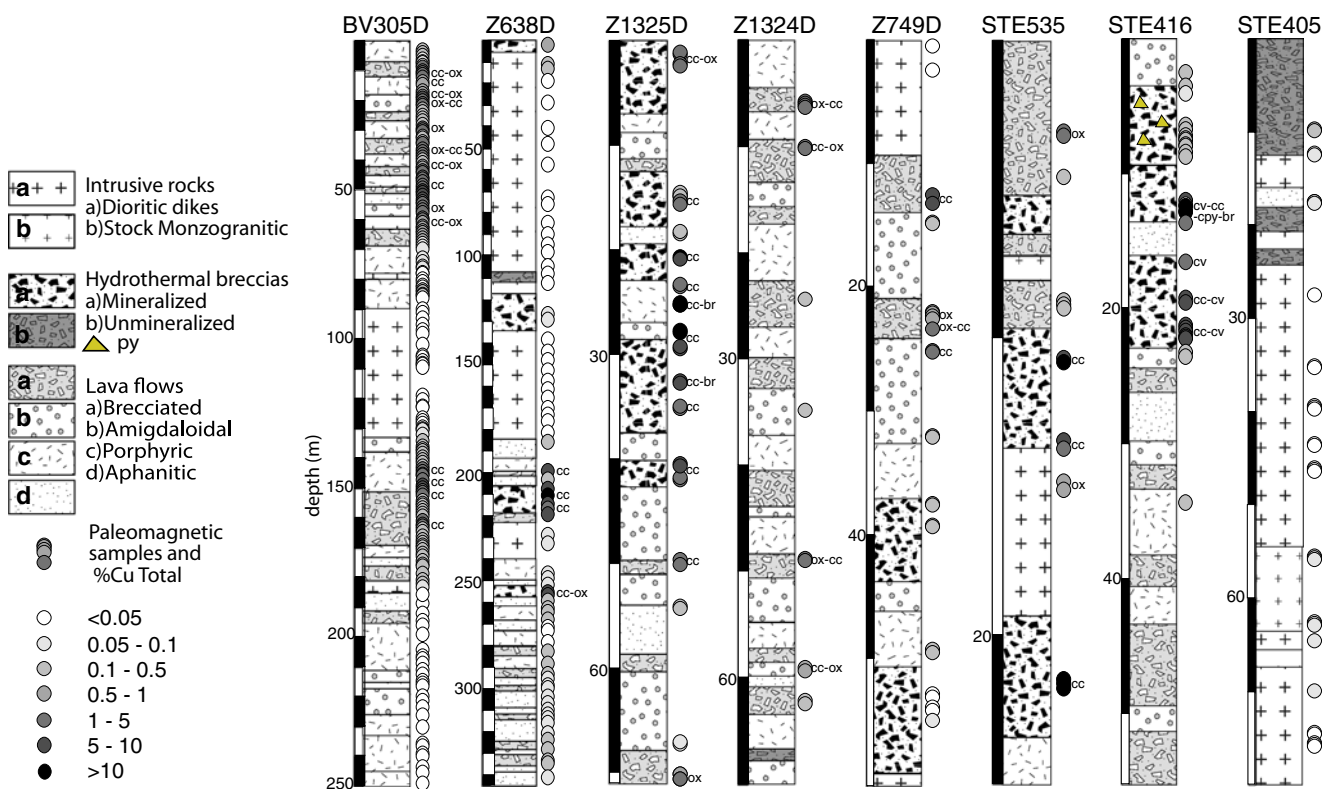


Fig. 4 Rock types, sample distribution, Cu grades, and ore mineralogy for selected drill holes

Regional paleomagnetic data for unmineralized rocks (Arriagada et al. 2003) provide a comparative baseline for the country rocks.

Paleomagnetic procedures and methodology

Nine sites were sampled with a hand-held drill in the Carolina de Michilla district. These minicore samples were oriented in situ with a solar (82%) or magnetic (18%) compass. Paleomagnetic minicore samples from the exploration drill cores were taken with a mounted electric drill by drilling perpendicular to the exploration drill core axis, taking care to register accurately the up-down direction of the core pieces by verifying that the core pieces had not been previously inadvertently inverted in the core boxes. The exploration drill cores are not oriented but their azimuth and inclination are known. The drill core STE405 is horizontal and almost E–W. This configuration does not allow recognition of normal and reverse polarity magnetizations, and therefore, this core was not used for determination of the characteristic remanent magnetization (ChRM).

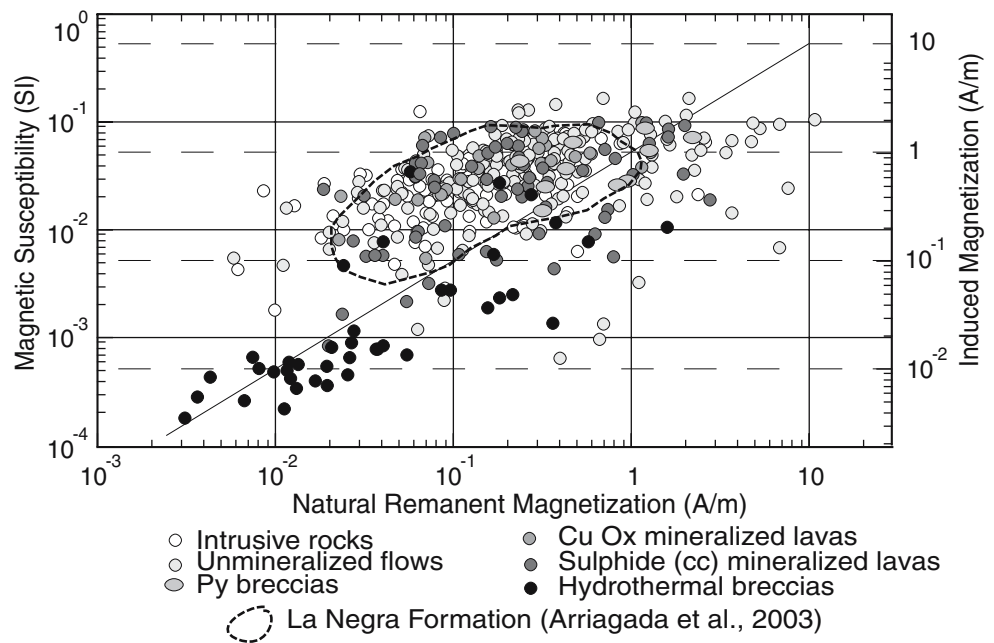
All samples were later cut to standard 2.2-cm long paleomagnetic samples. The NRM for each sample was measured with a Molspin (range 10^{-4} –100 A/m) or Agico

JR5A (range 10^{-5} –1500 A/m) spinner magnetometer. Additionally, volumetric magnetic susceptibility (k) was measured with a Bartington MS2 susceptibility meter.

Some samples from each site and representative samples from drill cores were demagnetized in four to ten steps of increasing alternating field (AF) with a Molspin demagnetizer. Several samples were also thermally demagnetized (eight to ten steps) in an ASC brand high capacity oven with a residual field of <10 nT in the cooling chamber. Characteristic remanent magnetization directions were determined by principal component analysis (Kirschvink 1980). After each thermal demagnetization step, susceptibility measurements were made to recognize mineralogical changes associated with the destruction of sulfide minerals by oxidation upon heating. Acquisition of isothermal remanent magnetization (IRM) tests were performed using an ASC brand pulse magnetizer, and an Agico KLY3/CS3 instrument was used to measure susceptibility from room temperature up to 700°C . Detailed descriptions of paleomagnetic procedures can be found in Butler (1992) and of rock magnetism in Dunlop and Özdemir (1997).

Representative samples from each site were taken from the same paleomagnetic core samples for thin-section preparation and lithologic alteration characterization. Details were described in the previous section and summarized in Tables 1 and 2.

Fig. 5 Logarithmic diagram of k versus J_0 differentiated by rock type for the Carolina de Michilla district samples. The induced magnetization was calculated using the present-day intensity of the Earth’s magnetic field near Michilla of about 20 A m^{-1} . The straight line corresponds to an equal contribution of induced and remanent magnetizations where the Koenigsberger ratio equals 1.0. The area enclosed by the dotted line represents the range of values for lavas of the La Negra Formation in the Tocopilla and Antofagasta sectors (Arriagada et al. 2003)



Magnetic properties

Most samples have high magnetic susceptibilities ($k > 0.01 \text{ SI}$) and relatively low NRM intensities ($J_0 < 1 \text{ A/m}$; Fig. 5); a pattern that was previously observed in the unmineralized La Negra volcanics near Tocopilla and Antofagasta (Arriagada et al. 2003). These ranges of values, in this study referred to as the “main group,” characterizes the unmineralized country rocks, including both lavas and intrusives.

Mineralized altered rocks of the Michilla district have k and NRM J_0 values that plot within a similar range to that of the main group. Lavas with predominantly hypogene mineralization (chalcocite–covellite) have average k and J_0 values that are slightly higher by less than one order of magnitude than those observed in sectors characterized by mixed mineralization (oxidized copper minerals and sulphides). In some cases, lavas with chalcocite mineralization give J_0 values that are larger than those of the main group and up to 3 A/m . Unmineralized lavas of the Michilla district plot on average within the main group field. In these unmineralized lavas, some samples from exploration drill hole EZ638D, taken close to the hydrothermal breccias, have k values in the order of 10^{-3} that are comparable to the k values in the breccias. Finally, copper-sulphide-bearing hydrothermal breccias have k values predominantly below 2×10^{-3} with J_0 values mostly between 3×10^{-3} and $5 \times 10^{-2} \text{ A/m}$ but with some up to 0.4 A/m . In exploration drill hole BV305, high J_0 values are observed only locally (Fig. 6) as, for example, below the intrusive at a depth range of 140–150 m.

Thermomagnetic experiments (Fig. 7) give Curie points near 580°C and indicate that magnetite is the main magnetic carrier. During IRM acquisition tests (Fig. 8), sulphide-mineralized hydrothermal breccia samples show slow nonsaturating acquisition of magnetization under increasing magnetizing field, a behavior that is typical of high coercivity minerals, likely hematite. This is consistent with the low k values for these rocks. Other rock types plot between a rapid saturation by 250 mT , typical of pure magnetite, and a slower gradual magnetization that is typical of hematite, indicating increasing proportions of hematite with respect to magnetite. The loss of susceptibility near 350°C observed in Fig. 7b is comparable to drops of susceptibility measured in samples at room temperature after heating (Fig. 9). Permanent loss of susceptibility implies mineral phase destruction, true for maghemite at 350°C , as inversion of maghemite to hematite starts at about $250\text{--}300^\circ\text{C}$, but not compatible for other magnetic minerals such as pyrrhotite at the same temperature. Moreover, the high magnetic susceptibility, up to 0.1 SI , observed in these samples associated with IRM saturation below 250 mT cannot be explained by the possible presence of pyrrhotite. The decrease in magnetic susceptibility after heating at 350°C is especially observed in the samples from exploration drill core BV305D (Fig. 9). To better define the spatial variability in the maghemite content in the two best-sampled exploration drill holes, magnetic susceptibilities were measured after heating at 250 and 350°C (Fig. 6). These experiments indicate that maghemite and magnetite are the main magnetic minerals in the lavas. There is no

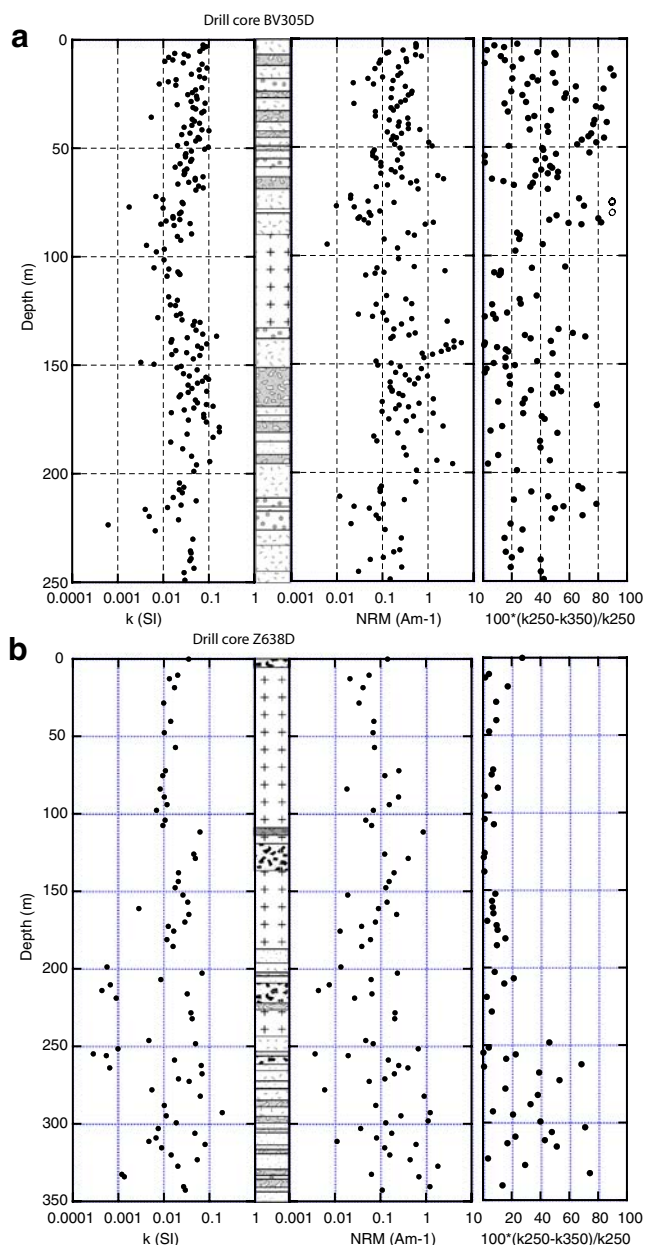


Fig. 6 Spatial variability of k and NRM for drill holes **a** BV305D and **b** Z638D. Zones of hydrothermal breccia (medium gray), sulfide (dark gray), and mixed (light gray) mineralization have been differentiated. During thermal demagnetization, a rapid decrease in magnetic susceptibility has been observed and attributed to inversion of maghemite to hematite. On the right side of the graphs, the variation in magnetic susceptibility between 250 and 350°C are plotted

magnetic evidence for maghemitization of the intrusive rocks in drill core Z638D.

Characteristic directions

Assuming that multiple mineralizing events spanned sufficient time to record opposite geomagnetic polarities, then the NRM should be the sum of antiparallel characteristic

remnant magnetizations. To detect such events and to analyze the nature and stability of NRM, several exploration drill core samples were stepwise demagnetized either thermally (TH) or by alternating fields to identify the characteristic components of the remanence. Only the magnetic inclination vector is relevant for the exploration drill cores because the paleomagnetic minicore samples were taken with no control on rotation of the exploration cores with respect to drill hole axis. However, to check for coherency and to detect possible drilling remanence overprints, more than one sample was taken with a common relative orientation.

Samples from the Lince open pit

Samples taken in situ from the Lince open pit correspond to the Cu-oxide level of mineralization. Magnetic susceptibility is high in most samples, and again, there are no major differences in the distribution of NRM intensities and magnetic susceptibilities when compared to the La Negra volcanics. NRM directions are strongly dispersed. Upon AF demagnetization, a soft component of magnetization with a normal polarity that likely corresponds to a Brunhes chron overprint (e.g., sample 00CM0101A, Fig. 10) is identified. Other samples seem to have a more stable secondary magnetization (Fig. 10). However, we were not able to identify a reliable pattern for the characteristic remanent magnetization in these samples (Fig. 10).

Drill core sampling

Mina buena vista Forty-four samples from drill core BV305 were AF demagnetized, and 27 were thermally demagnetized. Samples from this drill core are those that exhibit the largest susceptibility changes upon heating to about 300°C (Figs. 6, 9). There is, however, no clear relationship with the characteristic remanence direction because the susceptibility drop is not always related to a well-defined component of remanent magnetization (Fig. 11). Negative and positive inclinations are observed without a clear pattern along the profile. No stable magnetization was recovered in the intrusive rock intercepted at the depth interval of 90–120 m (Fig. 4). It is interesting to note that mineralized intercepts in mantoes from this drill hole have a stable magnetization with a low positive inclination (sample BV305D-148.6; Figs. 11, 12). The average mean inclination for the negative inclinations is steep (-55.7 ± 6.4) and in agreement with an overprint of the recent normal Earth's magnetic field (-40°), which, if adjusted for the azimuth and inclination of the exploration drill hole, becomes -60° in drill core coordinates.

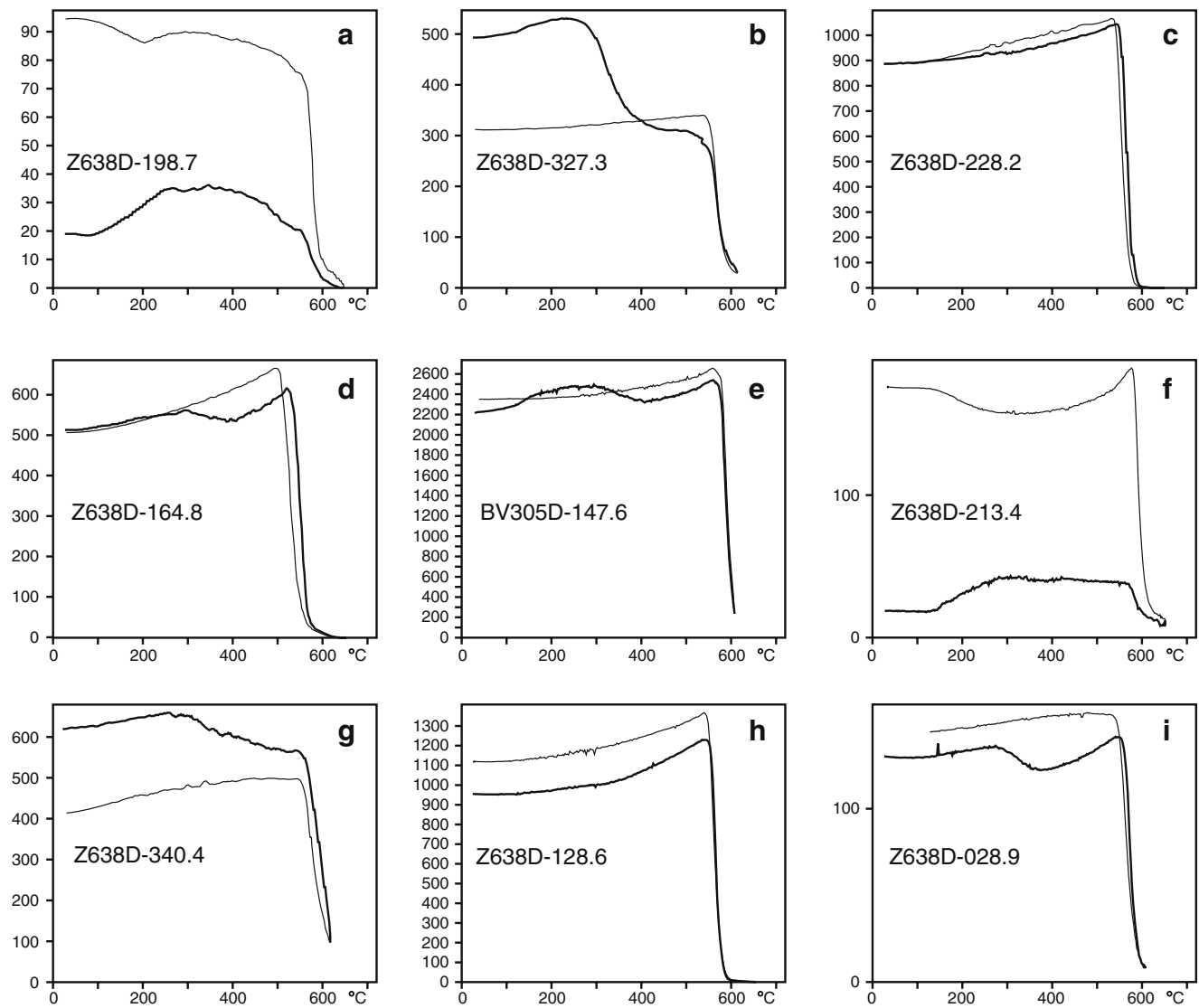


Fig. 7 Variation of magnetic susceptibility with temperature. Magnetite is the main magnetic mineral for samples with high magnetic susceptibility (c–e, g–i). Destruction of maghemite is observed in sample Z638D-327.3 (b). Formation of magnetite during heating is

observed in samples with low initial magnetic susceptibility (a, f). Thick (thin) lines correspond to the heating (cooling) curves. Magnetic susceptibility in arbitrary unit. All the experiments were performed with a similar sample volume

Mina lince–estefania Most samples from the hydrothermal breccias have univectorial magnetization with high unblocking temperatures between 450 and 600°C (Fig. 13). Samples with the lowest magnetic susceptibility also have a stable magnetization in the same temperature range, although their IRM acquisition suggests that hematite is the main magnetic mineral in samples with chalcocite or covellite. In several samples, an increase in magnetic susceptibility was observed during thermal demagnetization. Destruction of the sulfide minerals was likely by the reduction of hematite and the formation of new magnetite. The magnetizations of several samples with very high coercivity not demagnetized by AF demagnetization have unblocking temperatures in the range 550–590°C. Unblocking temperatures lower than the hematite Curie point of

675°C might be due partially to transformation upon heating during thermal demagnetization. The high stability of the magnetization during AF demagnetization may also be due to a contribution of single-domain magnetite together with hematite as magnetic carriers.

All samples with a stable remanent magnetization from other drill cores within this mine record positive inclinations (Figs. 12, 13). Magnetizations with a negative inclination are usually a soft unstable viscous remanent magnetization that was likely acquired in the recent Earth's field.

The characteristic mean remanent inclination in exploration drill core STE416 is $22.7 \pm 3.5^\circ$. It is slightly steeper in drill cores Z749D ($36.0 \pm 4.6^\circ$) and Z638D ($48.7 \pm 5.2^\circ$). In drill core Z638D, the characteristic directions with a positive

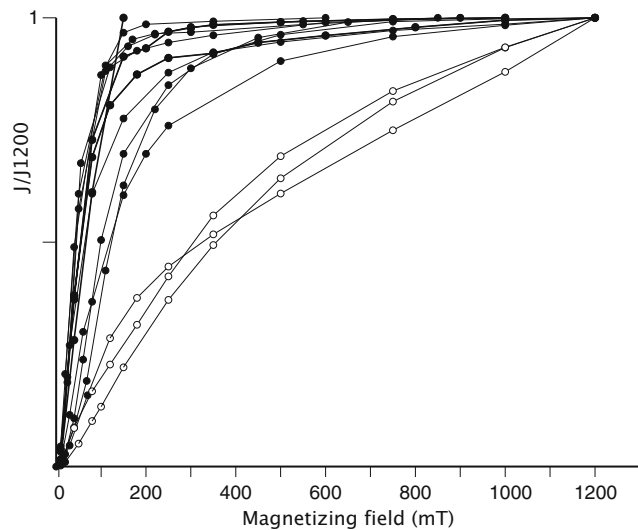


Fig. 8 IRM acquisition curves show the contribution of magnetite (filled circles) and hematite (open circles) with the latter being the main magnetic carrier in samples with low magnetic susceptibility. Some magnetite samples between the topmost trends and the hematite trends suggest a mixture of magnetite and hematite

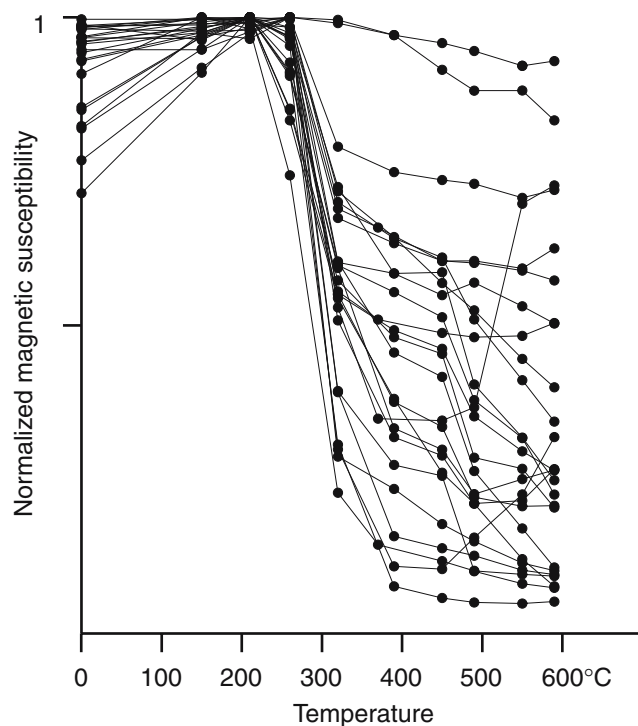


Fig. 9 Variation of magnetic susceptibility measured at room temperature, normalized to peak values, during progressive steps of thermal demagnetization for samples of drill core BV305D. A sharp drop in susceptibility is observed near 300°C. This is attributed to the inversion of maghemite to hematite

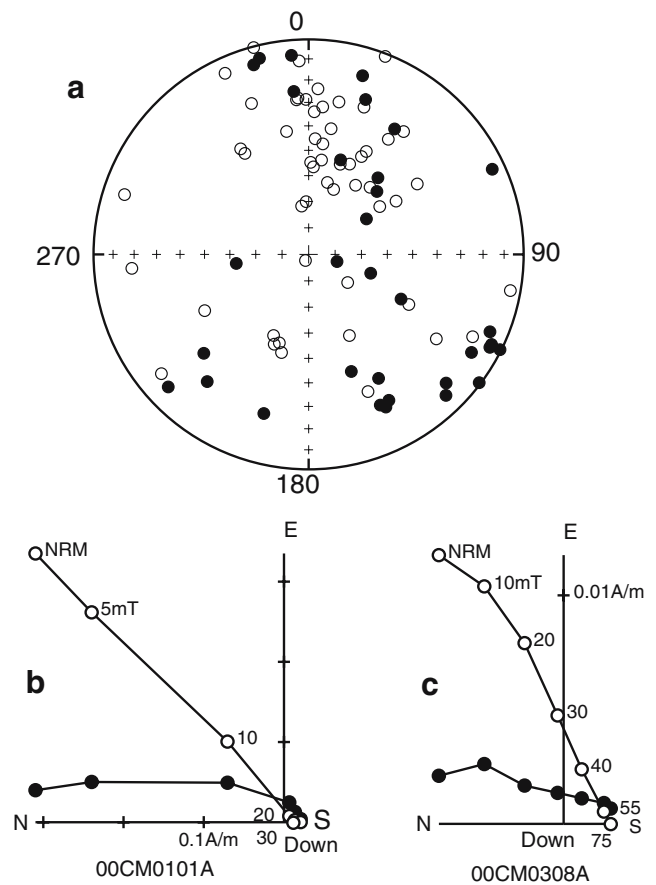


Fig. 10 a Equal-area stereo net of NRM directions for samples drilled in situ in the Lince open pit [open (solid) symbols correspond to the projection in the upper (lower) hemisphere and negative (positive) inclination]. b, c Orthogonal plots of AF demagnetization. Large secondary magnetizations with normal polarities are observed during AF demagnetization [b; open (solid) symbols correspond to the projection in the vertical (horizontal) plane]

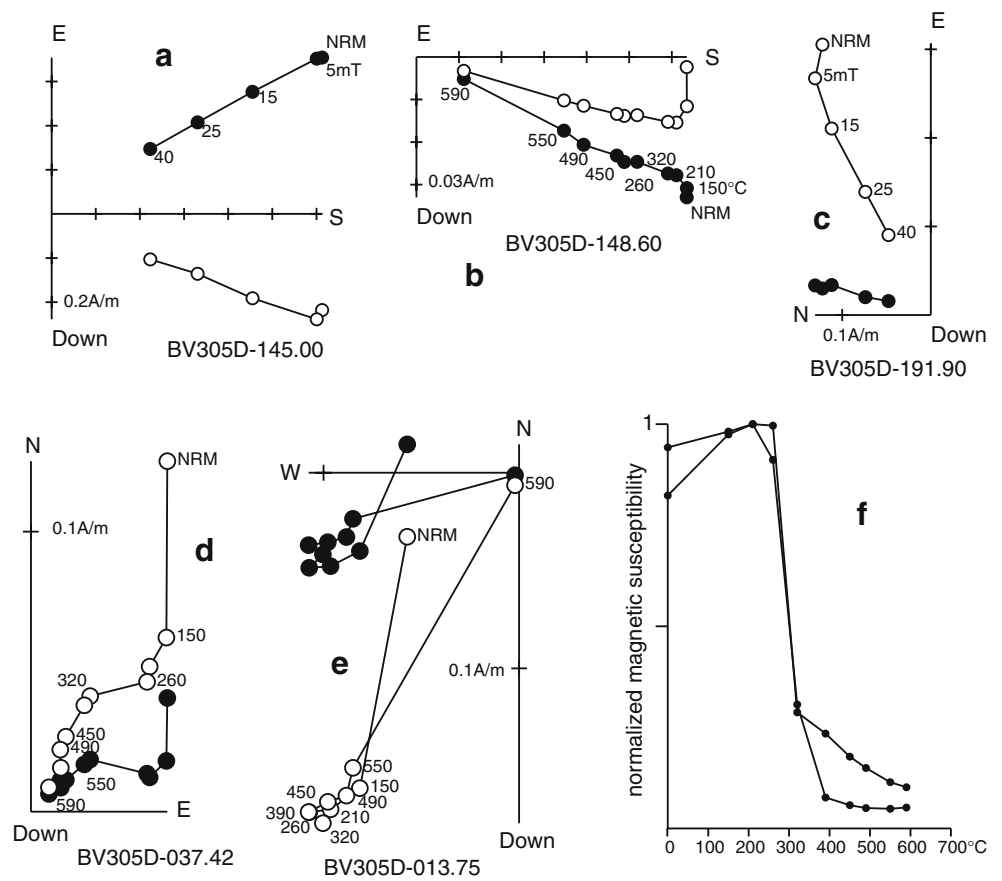
inclination are observed both in the thick intrusive body and in the lavas.

Discussion

Hydrothermal alteration

In broad terms, hydrothermal alteration in the Carolina de Michilla district, as described in this paper, is characterized by a quartz–albite–epidote–chlorite–calcite mineral assemblage overprinted by a regional “low-grade metamorphism/regional alteration” assemblage of quartz–epidote–chlorite–zeolites–pumpellyite–calcite (Losert 1973; Sato 1984; Espinoza et al. 1996; Venegas et al. 1991). Sulphide mineralized rocks show a local alteration assemblage of quartz–albite–gypsum, sometimes with feldspar-selective quartz–sericitic alteration. Both mineralization and hydrothermal breccias are commonly spatially related to dioritic intrusives with the hydrothermal alteration being subtly

Fig. 11 Representative AF (a, c) and thermal demagnetization data (b, d, e) for samples from drill core BV305D. Sample BV305D-148.6 has a highly stable component of magnetization. f Measurements of magnetic susceptibility at room temperature show a sharp drop in magnetic susceptibility in the temperature range 260–320°C for samples BV305D-037.42 and BV305D-013.75. This is interpreted as maghemite being the main magnetic mineral in these two samples. However, there is no corresponding well-defined component of magnetization in this temperature range [d, e; open (solid) symbols correspond to the projection in the vertical (horizontal) plane]



zoned with respect to the intrusives, going outward from actinolite–quartz–albite at the contact to quartz–albite–coarse epidote and then to quartz–fine epidote–chlorite, concentric with respect to the intrusive. Both mineralization and alteration in the host volcanic rocks are controlled by primary and secondary permeability that is associated with amygdales, breccias, and fractures.

In general, the alteration mineral assemblages fall within the so-called propylitic alteration category (Meyer and Hemley 1967) but, as proposed by Reed (1997), “propylitic alteration” has many subtleties and variations that deserve careful observation and classification. Mapping of alteration as “propylitic” provides little insight with respect to alteration zoning and possible vectors that point towards the source, especially when very little contrast is observed with the regionally altered rocks. Such is the case in the Carolina de Michilla district, hence, hydrothermal alteration, unless mapped in mineralogical detail, provides little information for exploration.

Figure 14 is a schematic cross-section of the Lince ore deposit where the alteration and mineralization effects are well constrained within narrow haloes around discrete mineralized mantoes and breccias. Alteration haloes, typically no wider than 100 m, contrast in mineralogy with respect to the observed mineral assemblage of unaltered lava rocks. The single most important alteration mineral is

albite, followed by epidote, and actinolite. These minerals contrast sharply against host-rock minerals such as chlorite, calcite, zeolite, prehnite, and pumpellyite.

Magnetic properties and hydrothermal alteration

The low-grade or regional metasomatism is responsible for the poor paleomagnetic record of the La Negra volcanics. The same observation was already made in the paleomagnetic study of the type sequence of the Jurassic volcanic rocks in Quebrada la Negra near Antofagasta (Arriagada et al. 2003). Maghemitization and partial to complete obliteration of the primary magnetic properties is most likely the product of the regional alteration.

In the magnetic susceptibility versus Cu plot for mineralized and unmineralized rocks (Fig. 15), a few samples with the highest Cu content show the lowest susceptibility values, while samples having high susceptibility values have varying degrees of copper content.

Regarding alteration and effects on magnetic mineralogy, IRM experiments indicate the presence of mostly hematite in the Cu–sulphide breccias. This is consistent with the low values of magnetic susceptibility in the breccias and with the observed mineralogy. All other rocks contain magnetite or maghemite. Except for the breccias having mostly hematite, it is impossible to magnetically distinguish

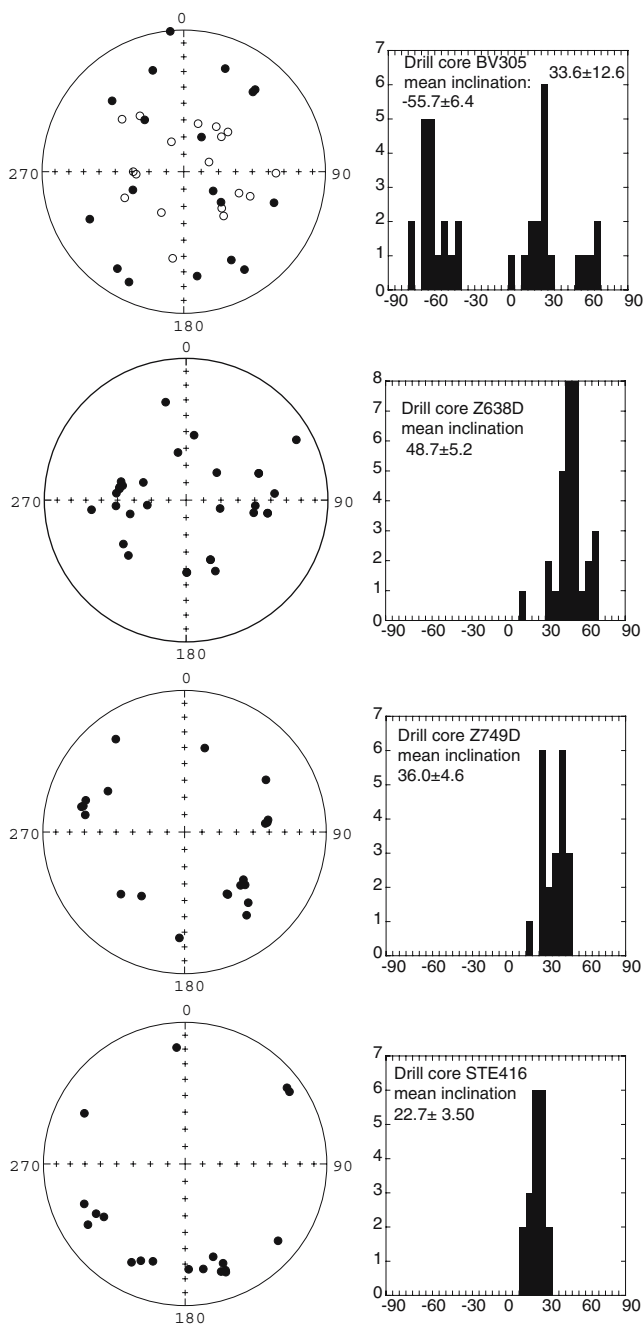


Fig. 12 Equal-area stereo nets showing the characteristic remanence directions in drill cores. High dispersion is observed in the Buena Vista Mine; two peaks with steep negative and positive inclinations were observed. There is a second peak with a low positive inclination. Characteristic directions for samples from the Lince–Estefania drill cores have positive inclinations in agreement with a major mineralisation event during a reverse polarity magnetic chron [*open* (*solid*) symbols correspond to the projection in the upper (lower) hemisphere]

mineralized bodies from unmineralized lavas, yet both pyrite-rich hydrothermal breccias and intrusives possess a more pure magnetite composition. The percentage of maghemite (%magh) in pyrite-rich hydrothermal breccias and intrusives is consistently low, as well as within Cu–

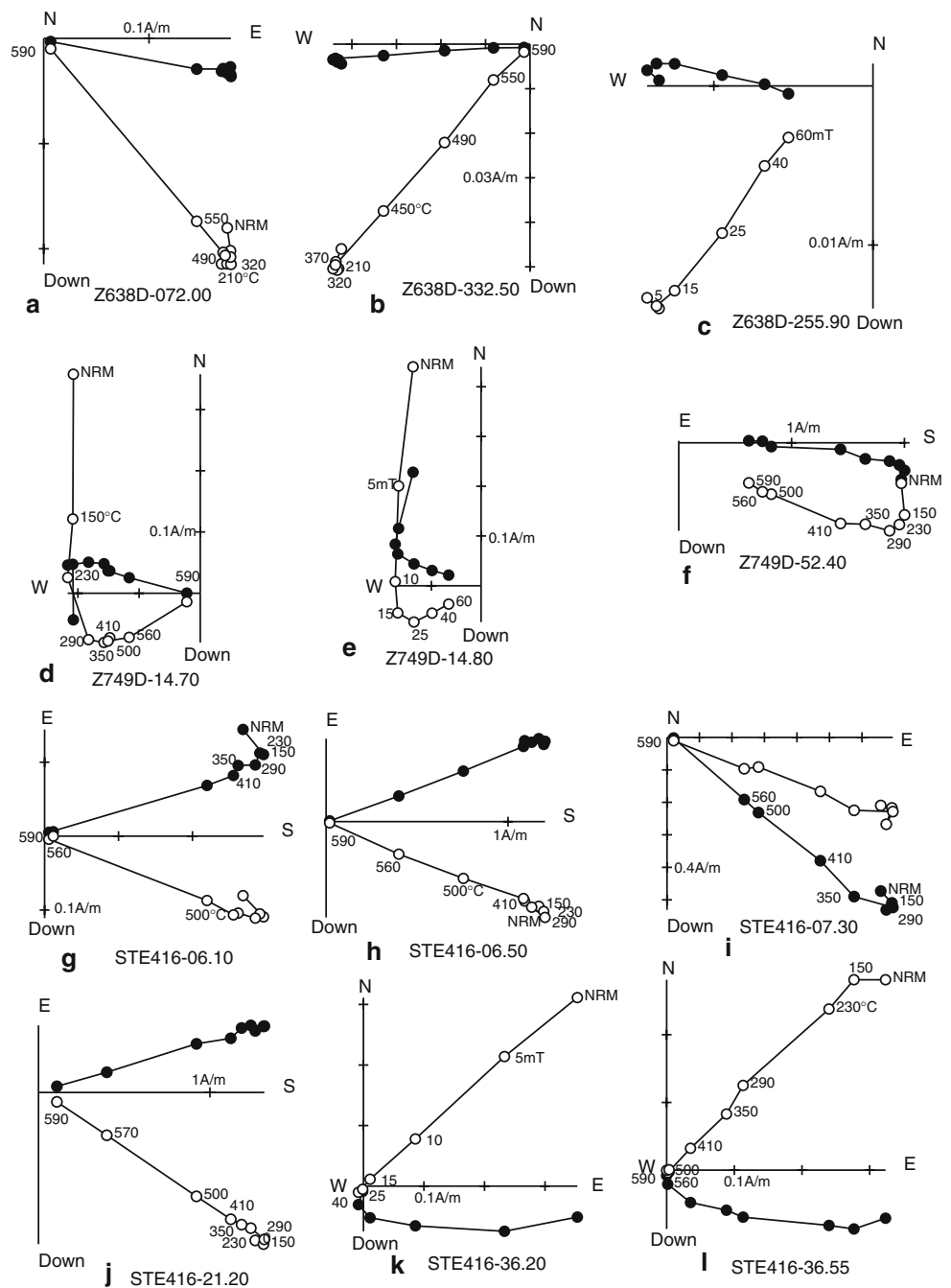
sulphide matrix breccias. This is partly corroborated by an observed inverse relation between Cu concentrations and % magh in two drill holes.

Finally, the overall effect of hydrothermal alteration on the paleomagnetic properties of the rocks is not clearly discernable, even at a small scale. This is consistent with the low contrast in mineralogy between the regional and hydrothermal alterations as described in this paper. The only exceptions are the Cu–sulphide hydrothermal breccias and their contact zones that have consistently low k and J_0 values. From an exploration point of view, magnetic exploration surveys are unlikely to discern mineralized bodies (Cu–sulphide breccias) except in a detailed ground magnetic survey because of the small size of these bodies. Structural discontinuities can most likely be determined, but exploration magnetic surveys are not recommended for the purpose of locating ore bodies.

Paleomagnetic considerations regarding age of mineralization

$^{40}\text{Ar}/^{39}\text{Ar}$ geochronologic data indicate ages of mineralization between 163 ± 2 and 137 ± 1 Ma (Oliveros 2005), which is in agreement with a Re/Os age of 159 ± 16 Ma (Tristá-Aguilera et al. 2005, 2006). Based on the following paleomagnetic consideration, an age of mineralization may be interpreted from data that is coeval with the currently known radiometric range. The exploration drill core STE416 is vertical. The characteristic remanence inclination recorded in this core is $22.7 \pm 3.5^\circ$. The Jurassic–Cretaceous boundary is a time of major change in the plate tectonics of the region. According to Besse and Courtillot (2002), the South American plate was at its lowest paleolatitude, around 145 Ma, and the expected inclination is only $\sim 30^\circ$. If the mineralization is slightly older at ~ 150 – 160 Ma, the expected inclination will be around $\sim 38^\circ$. If the age of the mineralization is in the range 140–145 Ma, we cannot discard the hypothesis that the mineralization occurred after a significant tilt of the volcanic sequence. Taking into account the results for the three exploration drill cores from the same mine (Fig. 16), the characteristic remanence direction should be common to all core samples. For unoriented exploration drill core, the characteristic remanence directions are distributed on a small circle about the drill hole axis orientation. The intersection of the three small circles from the three drill cores that have different dips and azimuths should correspond to the in situ characteristic direction. The apparent best solution (A, Fig. 16) indicates a declination of about 120° and low positive inclination (25°). The second most likely direction (solution B) corresponds to a declination of about 210° with an inclination near 30° . The flow beds are dipping nearly 45° toward the NNE. Such a correction leads the direction of solution A and B farther from the expected directions for a

Fig. 13 Selected thermal (a, b, d, f, g–j, l) and AF (c, e, k) demagnetization data for three drill cores of the Lince–Estefanía Mine. The characteristic remanent magnetization with a positive inclination has high unblocking temperatures 400–590°C (a, b, g–j). In sample Z749D-52.40 (f) a significant fraction of the characteristic magnetization is left above 590°C. The component of magnetization with a negative inclination (e.g., d, e, k) has a low unblocking temperature spectrum and does not intercept the origin during demagnetization. We interpret this magnetization component to be a secondary overprint. [open (solid) symbols correspond to the projection in the vertical (horizontal) plane]



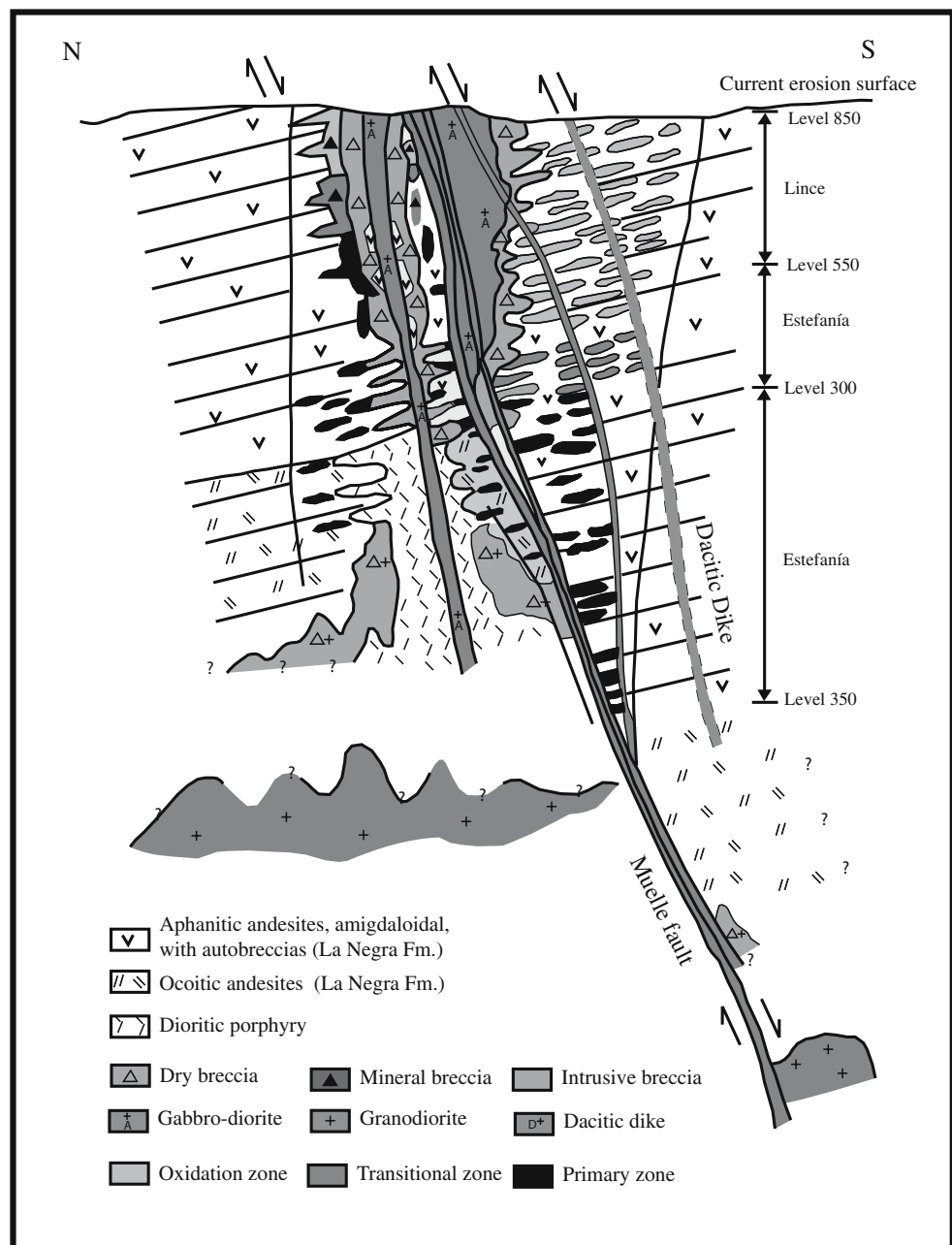
time interval 140–160 Ma than the one in situ coordinate. Applying a tilt correction to the direction in solution B leads to a steep inclination of $>70^\circ$.

Although some samples from natural outcrops in the intrusive rocks from the Michilla district are affected by lightning, we were able to obtain characteristic directions from several sites (Table 3). If we remove the data from site MC01 and MC02 for which we do not have a good constraint on the age, the mean results show clockwise rotations of 30 to 40° , depending on the age of the magnetization between 150 and 135 Ma (Fig. 16), supporting solution B observed in the drill cores. Clockwise block

rotations are an important tectonic feature of the early tertiary evolution of the northern Chilean forearc (Arriagada et al. 2003; Taylor et al. 2005).

The directions observed in the Pluton Viera are close to the B directions from the drill cores. Recent radiometric $^{40}\text{Ar}/^{39}\text{Ar}$ data (Oliveros 2005) provide an age of 145 Ma for the pluton, in good agreement with the low inclination expected for the south American plate (Besse and Courtillot 2002). Thus, we speculate that the characteristic direction recorded by the primary ore deposits is mostly a post-tectonic magnetization, suggesting a Late Jurassic–Early Cretaceous age for the copper mineralization.

Fig. 14 Schematic cross-section of the Susana ore deposit, depicting rock types, alteration, and mineralization distribution and mineralization zones. Hydrothermal alteration halos surrounding individual small ore bodies are too narrow to depict



Conclusions

Our detailed hydrothermal alteration, mineralization, and paleomagnetic study in the copper district of Carolina Michilla leads to the following conclusions.

1. Most rock units with or without strong hydrothermal alteration have a low ratio of NRM to induced magnetization intensity. Either hydrothermal and mineralization processes had no profound effect on the magnetic properties of the original host rock, or regional metasomatism overprinted and homogenized the mag-
2. On average, the magnetic susceptibility values are high, and there are no profound differences in the magnetic properties of the mineralized ore bodies and the La Negra volcanic formation that has been affected by low grade metamorphism or regional host-rock metasomatism. Only the mineralized hydrothermal breccias with covellite and bornite have a low magnetic susceptibility to give a measurable magnetic low anomaly for the

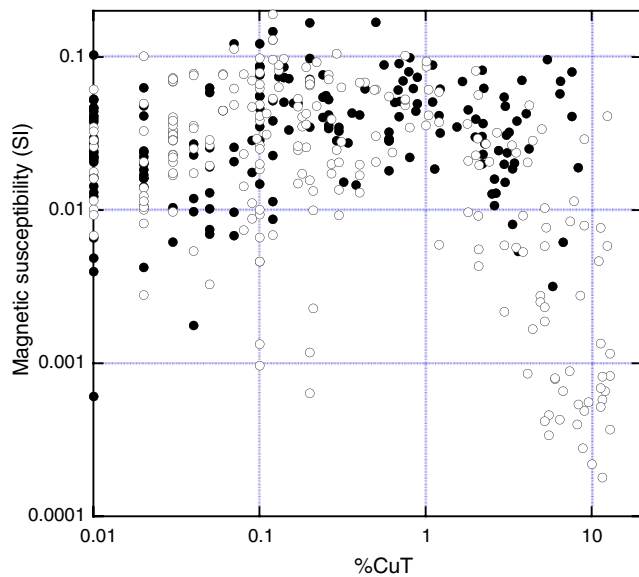


Fig. 15 Magnetic susceptibility versus Cu concentration. *Filled* symbols correspond to samples from drill cores BV305D, while *open* symbols are from drill cores of the Lince–Estefania Mine. Samples with low magnetic susceptibility have higher copper content

Table 3 Summary of paleomagnetic results

Site	Characteristic directions				
	<i>N</i>	Dec (degree)	Inc (degree)	α_{95} (degree)	<i>k</i>
MC01	5	201.0	49.3	5.6	190
MC02	7	90.6	−58.0	4.7	165
MC04	4	210.0	31.5	3.3	1,022
MC05	4	34.9	−39.3	12.0	216
MC06	5	32.7	−38.8	4.1	346
MC09	6	203.4	27.0	13.0	45
Mean	6	34.9	−42.4	17.0	17
Mean ^a	4	30.0	−34.2	8.3	124

N Number of samples; *Dec* and *Inc* declination and inclination of the characteristic remanent magnetization; α_{95} confidence angle at 95%; *k* Fisher (1953) concentration parameter

^a Mean calculated without MC01 and MC02

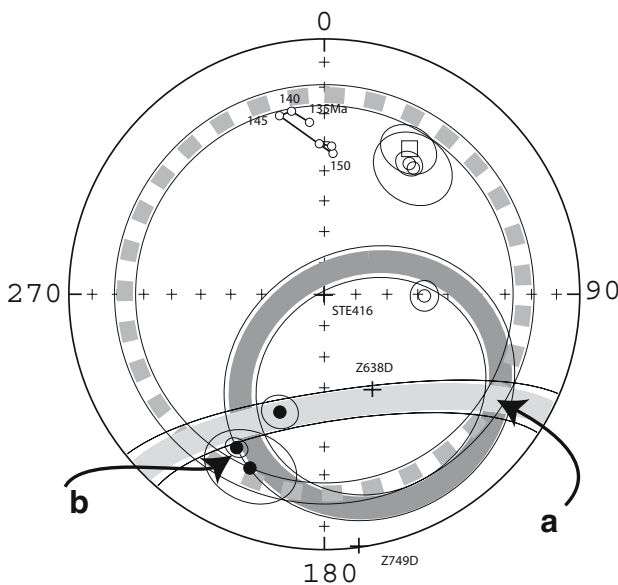


Fig. 16 Plot of the small circles with their bounding 95% confidence limits around the three exploration drill cores Z638D, Z749D, and STE416 (data in Fig. 13). *Open* and *filled* circles with cone of confidence at 95% are the ChRM directions of the sites within the Michilla district (Table 3). The square corresponds to the mean direction given in Table 3. Expected directions from the apparent polar wander path of Besse and Courtillot (2002) are shown with *small circles* and corresponding ages. The apparent best intersection of the *three small circles* of in situ coordinate is solution A. However solution B is more coherent with the results from the district than solution A

induced magnetization. The remanent magnetization is not intense enough to contribute significantly to the magnetic anomalies.

3. A characteristic remanent magnetization with a positive inclination was observed in drill cores within the primary mineralization of the Estefania mine. This magnetization component has high unblocking temperatures and is not easily AF demagnetized. Within exploration drill core Z638D, intrusive rock and mineralized lavas record the same polarity of magnetization, suggesting a genetic link between the intrusive stocks and mineralization. The paleomagnetic results are best explained by a short-lived mineralizing event related to the intrusion of the stocks during a time when the Earth’s geomagnetic field had a reversed polarity.
4. The intersection of the three small circles derived from the characteristic remanent inclination magnetizations in three exploration drill cores from the Estefania mine provide two possible characteristic remanent magnetization directions. However, one of these directions agrees far better with the directions observed in the in situ sites. The low inclination recorded by the characteristic directions from the mineralized mantoes is in good agreement with the low inclination recorded by the Viera Pluton that has a radiometric age of 145 Ma. This is also the time of a large cusp in the apparent polar wander path of the South American plate (Besse and Courtillot 2002; Schettino and Scotese 2005). If the age of the magnetization recorded by the primary ore is indeed near the Jurassic–Cretaceous boundary, then the paleomagnetic results suggest that the mineralization is mostly post-tectonic within the Michilla district.
5. The low contrast in the rock magnetic properties of mineralized and unmineralized rocks, except for small local ore bodies, indicate that regional and district

aeromagnetic surveys are unlikely to discern mineralized bodies from the host rock. Thus, such surveys are an exploration tool that is unsuited directly for finding covered sulfide ore deposits of the Michilla district type. This does not preclude the existence of magnetic contrasts associated with structural discontinuities such as faults. As both intrusives and ore deposits do have a spatial association with the prevailing fault systems, aeromagnetic data may discern such faults and their intersections, yet not pinpoint specific covered deposits.

Acknowledgment This research was funded by project DID I009/2, University of Chile, and by IRD–France. We thank J. Camacho, P. Sepulveda, and Minera Michilla for granting access and permission for research. We also thank Richard Naslund and Bill Blackburn at the University of New York, Binghamton, for help with the microprobe analysis.

References

- Acevedo J, Herrera H, Camacho J, Alfaro H (1997) Antecedentes y modelamiento geológico del yacimiento Susana, distrito minero Carolina de Michilla, II región de Antofagasta, Chile. *Actas VIII Congreso Geológico Chileno* 2:826–831
- Aguirre L, Féraud G, Morata D, Vergara M, Robinson D (1999) Time interval between volcanism and burial metamorphism and rate of basin subsidence in a Cretaceous Andean extensional setting. *Tectonophysics* 313:433–447
- Arriagada C, Roperch P, Mpodozis C, Dupont-Nivet G, Cobbold P, Chauvin A, Cortés J (2003) Paleogene clockwise tectonic rotations in the forearc of central Andes, Antofagasta region, northern Chile. *J Geophys Res* 108(B1):2032
- Besse J, Courtillot V (2002) Apparent and true polar wander and the geometry of the geomagnetic field over the last 200 Myr. *J Geophys Res* 107(B11):2300
- Boric R, Díaz F, Maksiav V (1990) Geología y yacimientos metalíferos de la región de Antofagasta. Servicio Nacional de Geología y Minería, bol. 40. Servicio Nacional de Geología y Minería, Santiago, Chile
- Buchelt M, Tellez C (1988) The Jurassic la Negra formation in the area of Antofagasta, northern Chile (lithology, petrography, geochemistry). In: Bahlburg H, Breitzkreuz C, Giese P (eds) *The southern central Andes*. Springer, Heidelberg, Germany, pp 171–182
- Butler RF (1992) *Paleomagnetism: magnetic domains to geologic terranes*. Blackwell, Oxford, UK
- Dunlop DJ, Özdemir Ö (1997) *Rock magnetism: fundamentals and frontiers*. Cambridge University Press, Cambridge
- Espinoza S, Véliz H, Esquivel J, Arias J, Moraga A (1996) The Cupriferous province of the coastal range, northern Chile. In: Camus F, Sillitoe R, Oettersen R (eds) *Andean copper deposits: new discoveries, mineralization, styles and metallogeny*. Society of Economic Geologists Special Publication 5:19–32
- Fisher RA (1953) Dispersion on a sphere. *Proc Royal Soc London* 217A:295–305
- García F (1967) Geología del norte grande de Chile. Simposio geosinclinal andino, no. 3. Sociedad Geológica de Chile, Santiago, Chile
- Kirschvink JL (1980) The last-squares line and plane and the analysis of paleomagnetic data. *Geophys J R Astron Soc* 62:699–718
- Losert J (1973) Alteration and associated copper mineralization in the Jurassic volcanic rocks of the Buena Esperanza mining area (Antofagasta province, Northern Chile). *Departamento de Geología Universidad de Chile* 41:51–85
- Maksiav V (2000) Significado tectónico y metalogénico de datos de trazas de fisión en apatitas de plutones de la Cordillera de la Costa de la región de Antofagasta. *Actas IX Congreso Geológico Chileno* 2:129–134
- Maksiav V, Zentilli M (2002) Chilean stratabound Cu–(Ag) deposits: an overview. In: Porter TM (ed) *Hydrothermal iron oxide copper–gold and related deposits: a global perspective*, 2. PCG Publishing, Adelaide, pp 185–205
- Marinovic N, Smoje I, Maksiav V, Hervé M, Mpodozis C (1995) Hoja Aguas Blancas, Región de Antofagasta. *Carta Geológica de Chile*, no. 70. Servicio Nacional de Geología y Minería, Santiago
- Meyer C, Hemley J (1967) Wall rock alteration. In: Barnes HL (ed) *Geochemistry of hydrothermal ore deposits*. Holt, Rinehart and Winston, New York, pp 166–235
- Muñoz N, Venegas R, Tellez C (1988) La Formación La Negra: Nuevos antecedentes estratigráficos en la Cordillera de la Costa de Antofagasta. *Actas V Congreso Geológico Chileno* 1:43–55
- Naranjo J, Puig A (1984) Hojas Taltal y Chañaral, regiones de antofagasta y atacama. *Carta geológica de Chile*, no. 62–63, Escala 1:250.000. Servicio Nacional de Geología y Minería, Santiago
- Niemeyer H, Standen R, Venegas R (1990) Proyecto de exploración geológica distrital, geología del distrito minero Carolina de Michilla. Superintendencia de geología, Michilla Mining Company 1, 2:381p
- Oliveros V (2002) Eventos de alteración en las rocas ígneas del distrito minero de Michilla, II región, Chile: relación con la mineralización de cobre. M.Sc. thesis, Departamento de Geología, Universidad de Chile
- Oliveros V (2005) Étude géochronologique des unités magmatiques Jurassiques et Crétacé inférieur du Nord du Chili (18°30′–24°S, 60°30′–70°30′W): Origine, mise en place, altération, métamorphisme et mineralizations associées. Dissertation, Université de Nice-Universidad de Chile
- Palacios C (1986) Subvolcanic copper deposits in the coastal range of northern Chile. *Zbl Geol Palaönt Teil* 1(9/10):1605–1615
- Palacios C, Definis A (1981) Geología del yacimiento estratiforme “Susana”, Distrito Michilla, Antofagasta. *Proc of the 1st colloquia on volcanism and metallogenesis, Antofagasta*, pp 80–91
- Reed M (1997) Hydrothermal alteration and its relationship to ore fluid composition. In: Barnes KL (ed) *Geochemistry of hydrothermal ore deposits*. Wiley, pp 303–366
- Rogers G (1985) A geochemical traverse across the north Chilean Andes. Dissertation, Open University, United Kingdom
- Roperch P, Chauvin A (1997) Propiedades magnéticas de las rocas volcánicas de Chile e interpretación de las anomalías magnéticas. *Actas VIII Congreso Geológico Chileno, Antofagasta, Chile* 1:790–794
- Sato T (1984) Manto type copper deposits in Chile, a review. *Bulletin of the geological survey of Japan* 35:565–582
- Schettino A, Scotese CR (2005) Apparent polar wander paths for the major continents (200 Ma to the present day): a palaeomagnetic reference frame for global plate tectonic reconstructions. *Geophys J Int* 163:727–759
- Soto H, Dreyer H (1985) Geología de “Mina Susana”: un yacimiento novedoso en Carolina de Michilla. *IV Congreso Geológico Chileno. Actas IV Congreso Geológico Chileno* 2:335–338
- Taylor GK, Dashwood B, Grocott J (2005) Central Andean rotation pattern: evidence from paleomagnetic rotations of an anomalous domain in the forearc of northern Chile. *Geology* 33:777–780
- Tristá-Aguilera D, Barra F, Ruiz J, Morata D, Talavera-Mendoza O, Kojima S, Ferraris F (2006) Re–Os isotope systematics for the Lince–Estefanía deposit: constraints on the timing and source of

- copper mineralization in a stratabound copper deposit, Coastal Cordillera of Northern Chile. *Miner Deposita* 41:99–105
- Tristá-Aguilera D, Ruíz J, Barra F, Morata D, Talavera-Mendoza O, Kojima S, Ferraris F (2005) Origin and age of Cu-stratabound ore deposits: Michilla district, northern Chile. In: Proc VI International symposium on andean geodynamics, Barcelona, Spain, pp 742–745
- Venegas R, Vergara M (1985) Yacimientos de Fe–Cu–(Au) ligados a rocas intrusivas y volcánicas jurásicas de la Cordillera de la Costa a la latitud de Mejillones, II región de Antofagasta. *Actas IV Congreso Geológico Chileno* 3:3-730–3-751
- Venegas R, Munizaga F, Tassinari C (1991) Los yacimientos de Cu–Ag del distrito Carolina de Michilla, región de Antofagasta, Chile: nuevos antecedentes geocronológicos. *Actas VI congreso Geológico Chileno* 1:452–455
- Vivallo W, Henríquez F (1998) Génesis común de los yacimientos estratoligados de cobre del Jurásico medio a superior en la Cordillera de la Costa, Región de Antofagasta, Chile. *Revista Geológica de Chile* 25(2):199–228
- Wolf F, Fonboté L, Amstutz G (1990) The Susana copper (–silver) deposit in Northern Chile. Hydrothermal mineralization associated with a Jurassic volcanic arc. In: Fonboté L, Amstutz G, Cardozo M, Cedillo C, Frutos J (eds) Stratabound ore deposits. Society for Geology Applied to Mineral Deposits Special Publication 8:319–338